Electronic Supplementary Material (ESI) for Chemical Communications.

Supplementary Information

Tunable Deep-Blue Luminescence from Ball Milled Chlorine-Rich $Cs_x(NH_4)_{1-x}PbCl_2Br$ Nanocrystals by Ammonium Modulation

Hongfei Xiao,[a,b] Hao Xiong,[b] Ping Li,[b] Linqin Jiang,*[b] Aijun Yang,[c] Lingyan Lin,[b] Zhenjing Kang,[b] Qiong Yan,[a,b] and Yu Qiu*[b]

[a] College of Physics and Information Engineering, Fuzhou University, Fuzhou 350108, China

[b] Key Laboratory of Green Perovskites Application of Fujian Provincial Universities, College of Electronics and Information Science, Fujian Jiangxia University, Fuzhou 350108, China

[c] PV Metrology Institute, Fujian Metrology Institute, Fuzhou 350003, China

*Corresponding authors. Email: yuqiu@fjjxu.edu.cn; linqinjiang@fjjxu.edu.cn

Experimental section:

Materials:

Lead dichloride ($PbCl_2$, energy chemical, 99%), Cesium bromide (CsBr, Advanced Ejection Technology, 99.999%), Ammonium bromide (NH_4Br, Sinopharm), Oleylamine (OAm, Aladdin, 267.49MW) were used directly without further treatment.

Preparation:

Synthesis of perovskite powders: $PbCl_2$, CsBr and NH_4Br were mixed according to the designed molar ratios and placed in a 50 ml agate grinding jar together with 100ul of OAm. The total mass of the raw material was roughly 1.2g. Then, the powders were ground using a planetary ball-mill (Changsha MITR Corp., YXQM-4L) at the speed of 350 rpm for 2h in air.

Preparation of perovskite nanocrystal (PNC) solutions: 70 mg of the as-milled powder was dispersed in 70 ml of n-hexane with ultrasonication or stirring for 1h. The as-prepared milky liquid was centrifuged at 7000 rmp for 10min to obtain a clear PNC solution.

Characterization:

The Rigaku Ultima IV X-ray Diffractometer with Cu Kα source (λ = 1.5418 Å) was used to record the powder X-ray diffraction (XRD) patterns. The scanning electron microscopy (SEM) images were recorded on a scanning electron microscope (Helios G4 CX). The X-ray photoelectron spectra (XPS) of the samples were measured using a ESCALAB 250 XPS instrument. Ultraviolet-visible (UV-vis) absorption spectra were measured using SHIMADZU UV-2600 at room temperature. The photoluminescence (PL) spectra recorded at excitation of 365 nm were performed by Edinburgh FS5 transient steady-state fluorescence spectrometer. The time-resolved PL curves were determined with the same fluorescence spectrometer. The TECNAI G2 F20 transmission electron microscope (TEM) was used to record the TEM and high-resolution TEM (HRTEM) images of the PNCs.

XPS Results and Discussion:

The survey X-ray photoelectron spectroscopy (XPS) spectra confirm the existence of Cs, Pb, Cl, Br, O, C and N (Fig. S6, ESI$^+$). All samples exhibited a C 1s peak at 285.6 eV, which was attributed to the aliphatic carbon in OAm.[1] The weak O 1s was observed due to the adsorption of the ambient air. The N 1s peak can be divided into two subpeaks (Fig. S7, ESI$^+$) at 402.1 and 402.7 eV, pointing to the presence of N–H groups arising from the surface OAm ligand[1] and the lattice NH_4^+.[2] With the increase in the NH_4^+ content, the intensity of the subpeak at 402.7 eV grew gradually. The high-resolution Cs 3d spectra of $CsPbCl_2Br$ (Fig. S8, ESI$^+$) showed two distinct peaks of $3d^{3/2}$ and $3d^{5/2}$ at 738.8 and 724.8 eV, respectively.[3] The Cs 3d peaks of mixed $Cs_x(NH_4)_{1-x}PbCl_2Br$ shifted to lower binding energies slightly with the substitution of Cs by NH_4^+. On the other hand, the Pb $4f^{5/2}$ and $4f^{7/2}$ peaks of $Cs_x(NH_4)_{1-x}PbCl_2Br$ in Fig. S9 (ESI$^+$) showed an opposite trend, shifting to higher binding energies with the incorporation of NH_4^+. These results suggest the change of the chemical environment of Cs and Pb ions after the NH_4^+ doping. The locations of Cl $2p^{1/2}$, Cl $2p^{3/2}$, Br

$3d^{3/2}$ and Br $3d^{5/2}$ peaks seemed almost independent on the doping amount of NH_4^+ in mixed $Cs_x(NH_4)_{1-x}PbCl_2Br$, but shifted to higher binding energies for pure NH_4PbCl_2Br (Fig. S10 and S11, ESI^+).

References:

1 Y. Hou, Z. R. Zhou, T. Y. Wen, H. W. Qiao, Z. Q. Lin, B. Ge, H. G. Yang, *Nanoscale Horiz.,* 2019, **4**, 208-213.

2 M. Thompson, A. D. Nunn, E. N. Treher, *Anal. Chem.,* 1986, **58**, 3100-3103.

3 Y. Yu, G. Shao, L. Ding, H. Zhang, X. Liang, J. Liu, W. Xiang, *J. Rare Earth.,* 2021, **39**, 1497-1505.

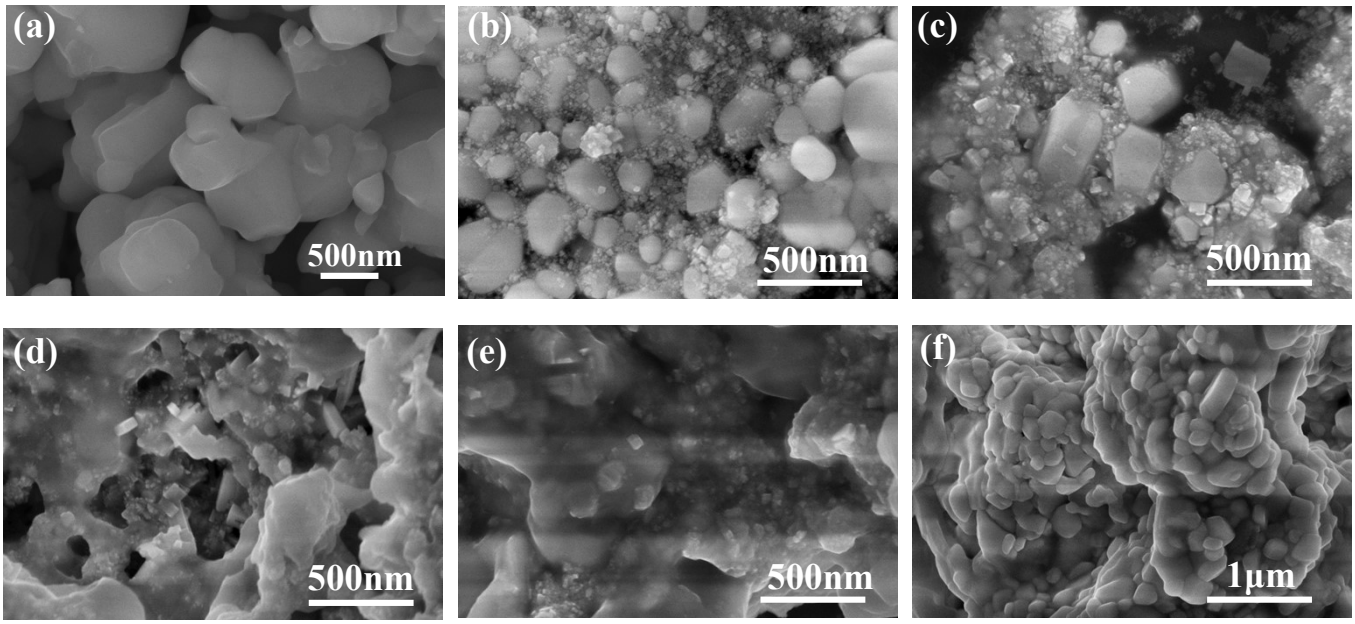

Figure S1. The SEM images of (a) $CsPbCl_2Br$ powder synthesized without OAm ligand and (b) $CsPbCl_2Br$, (c) $Cs_{0.3}(NH_4)_{0.7}PbCl_2Br$, (d) $Cs_{0.5}(NH_4)_{0.5}PbCl_2Br$, (e) $Cs_{0.3}(NH_4)_{0.7}PbCl_2Br$ and (f) NH_4PbCl_2Br powders synthesized with OAm ligand, respectively.

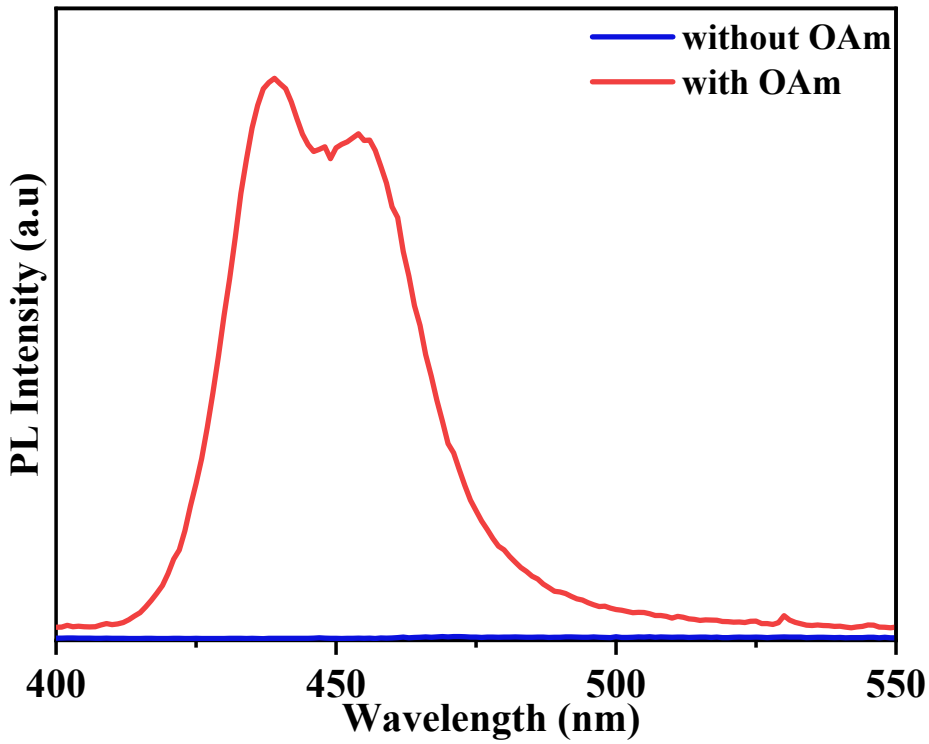

Figure S2. The PL spectra of $CsPbCl_2Br$ powders synthesized with and without OAm.

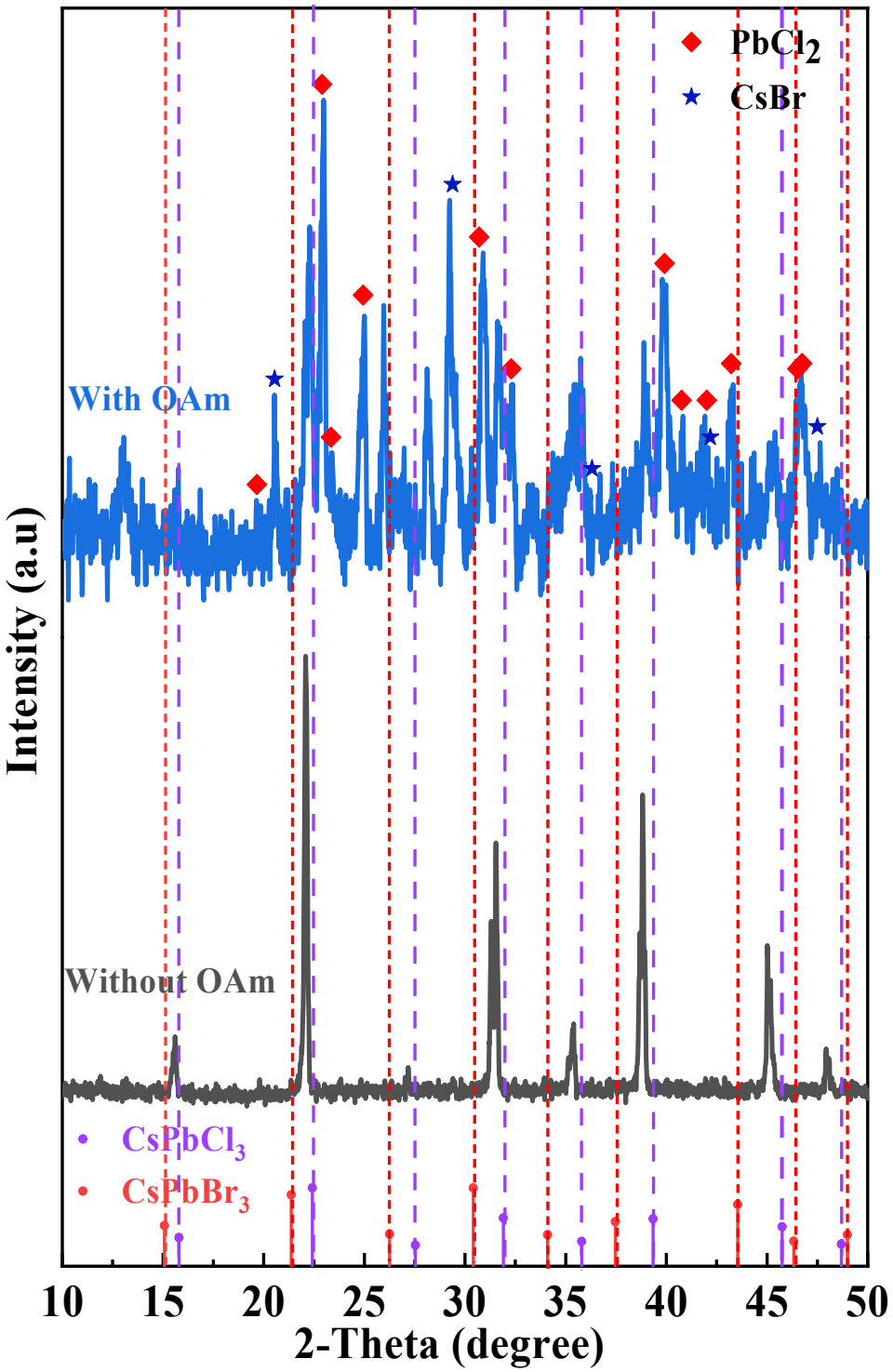

Figure S3. The XRD patterns of $CsPbCl_2Br$ powders prepared with and without OAm. The standard X-ray diffraction pattern of $CsPbCl_3$ (PDF 75-0412) and $CsPbBr_3$ (PDF 73-0692) are presented for comparison.

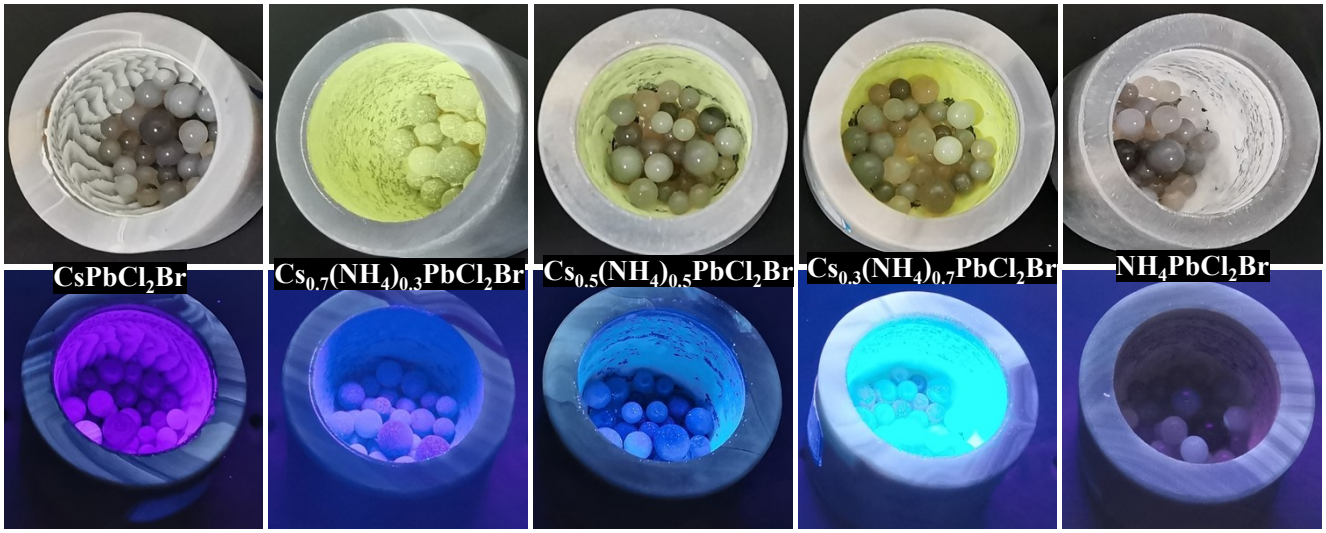

Figure S4. The optical photographs of as-milled $CsPbCl_2Br$, $Cs_{0.3}(NH_4)_{0.7}PbCl_2Br$, $Cs_{0.5}(NH_4)_{0.5}PbCl_2Br$, $Cs_{0.3}(NH_4)_{0.7}PbCl_2Br$ and NH_4PbCl_2Br powders under natural light indoors (upper images) or under 365 nm UV light (lower images).

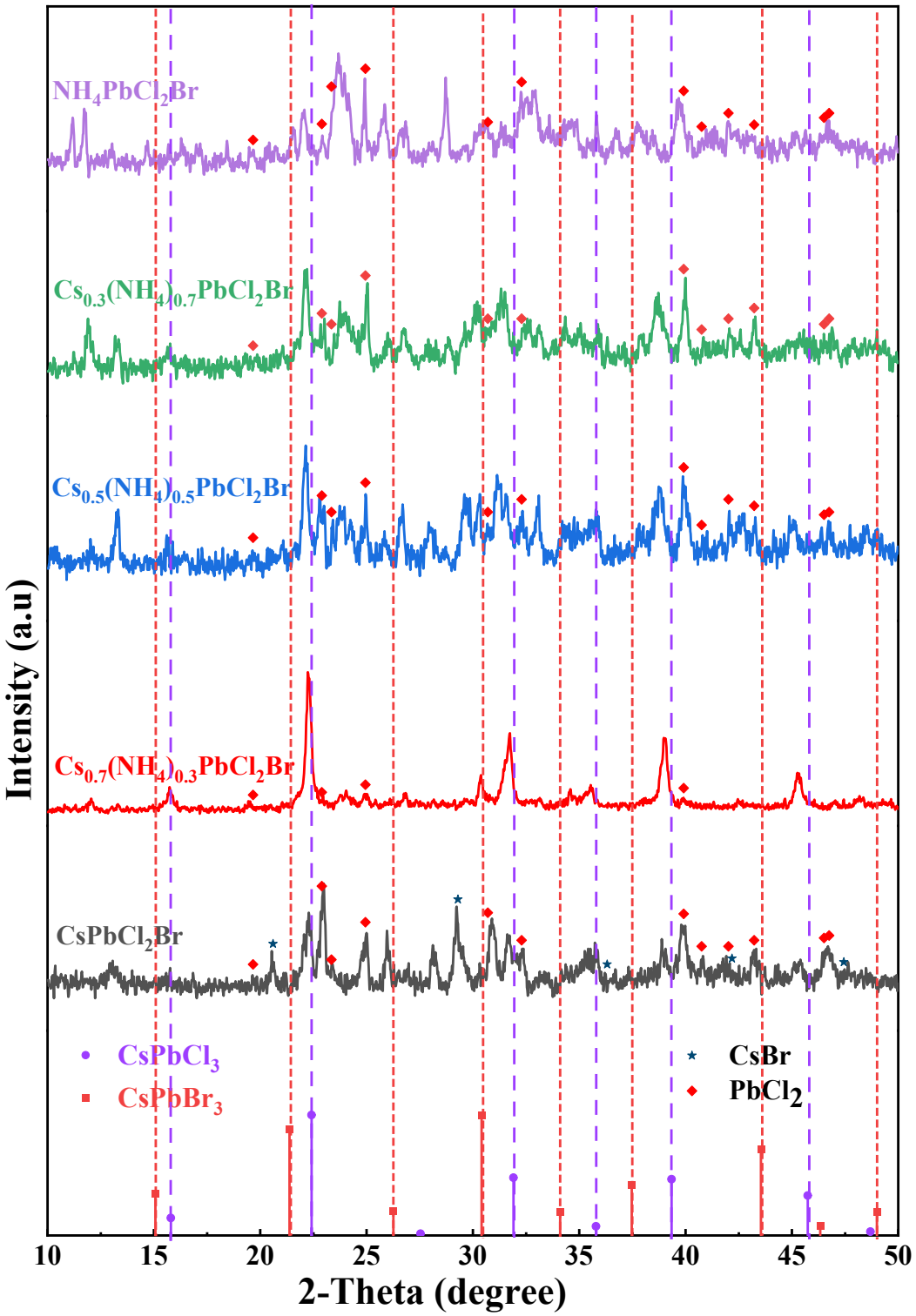

Figure S5. The XRD patterns of $Cs_x(NH_4)_{1-x}PbCl_2Br$ (x = 1, 0.7, 0.5, 0.3, 0) powders milled with OAm ligand. The standard X-ray diffraction pattern of $CsPbCl_3$ (PDF 75-0412) and $CsPbBr_3$ (PDF 73-0692) are presented for comparison.

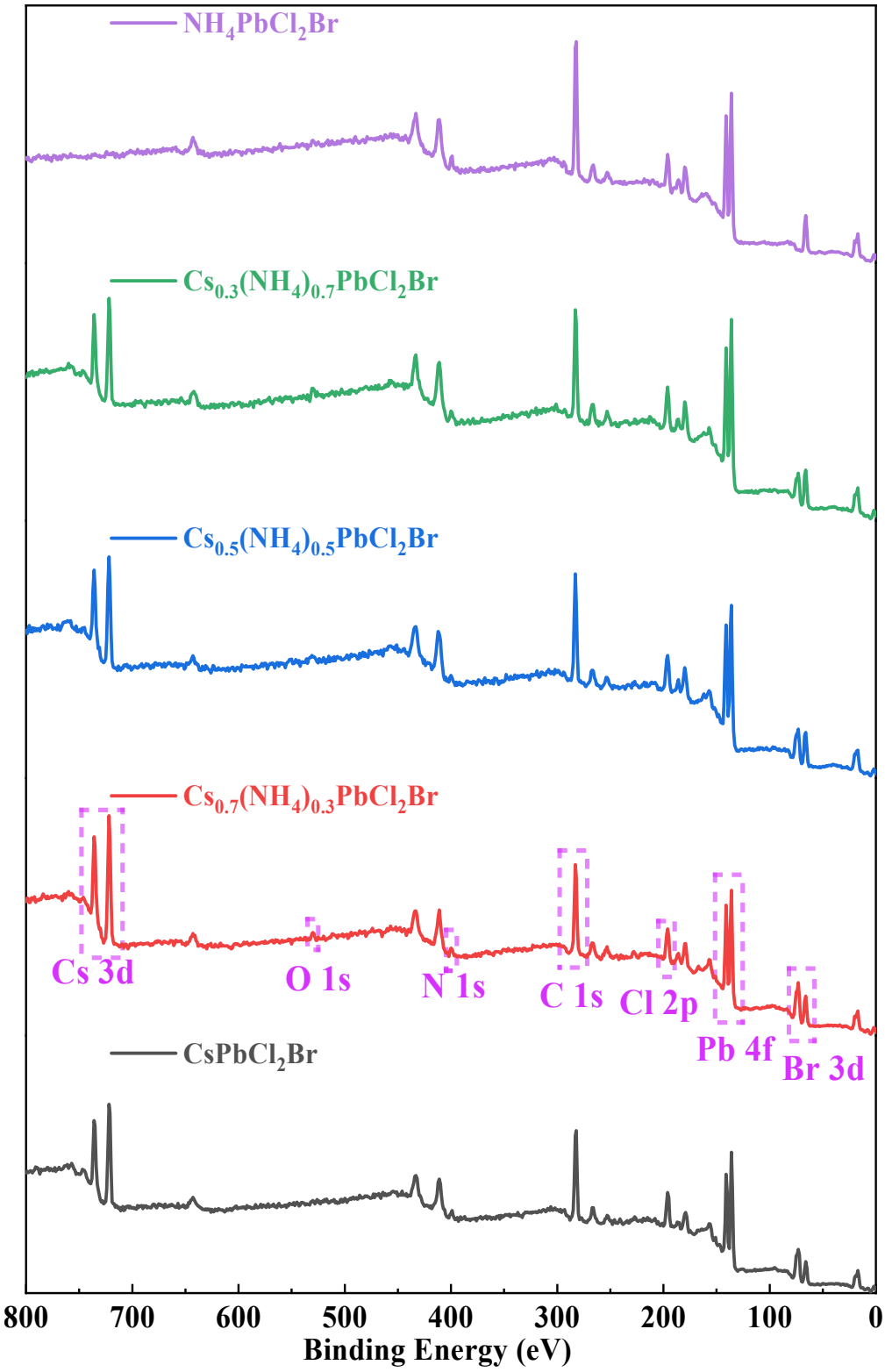

Figure S6. The XPS survey spectra of $Cs_x(NH_4)_{1-x}PbCl_2Br$ (x = 1, 0.7, 0.5, 0.3, 0) powders.

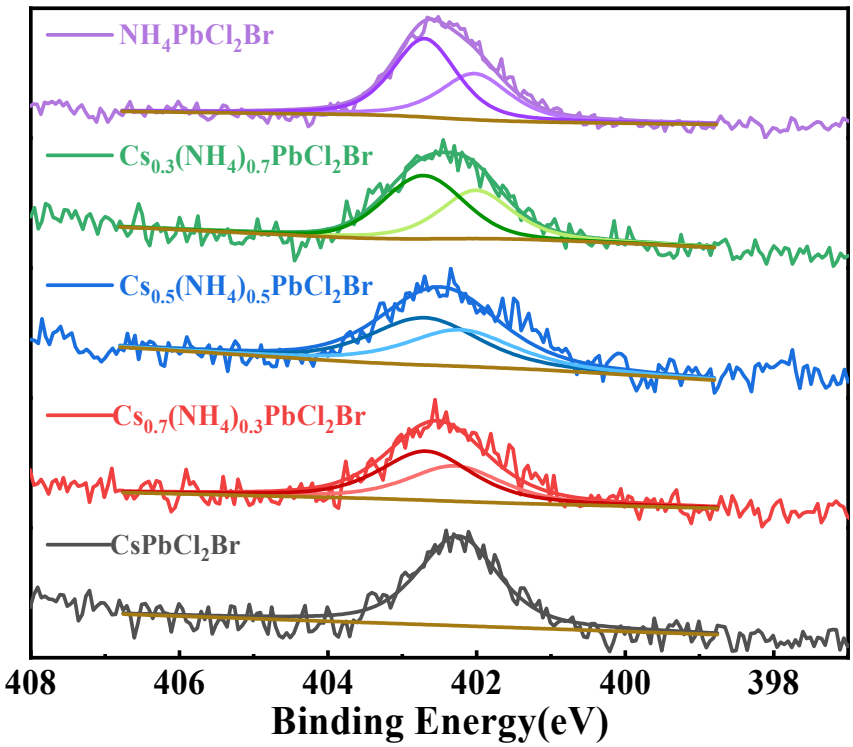

Figure S7. High-resolution N 1s XPS spectra of $Cs_x(NH_4)_{1-x}PbCl_2Br$ (x = 1, 0.7, 0.5, 0.3, 0) powders.

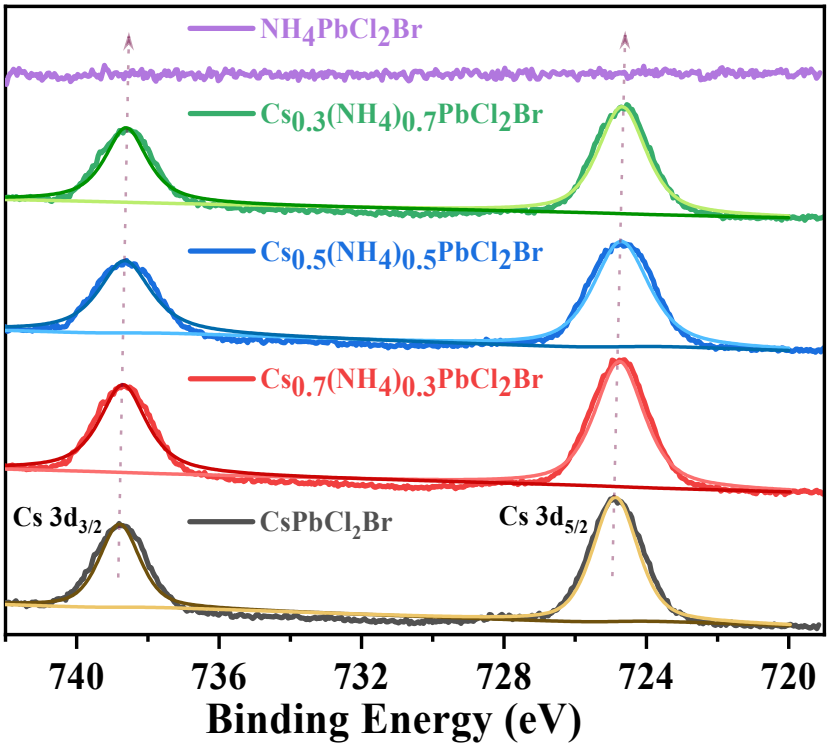

Figure S8. High-resolution Cs 3d XPS spectra of $Cs_x(NH_4)_{1-x}PbCl_2Br$ (x = 1, 0.7, 0.5, 0.3, 0) powders.

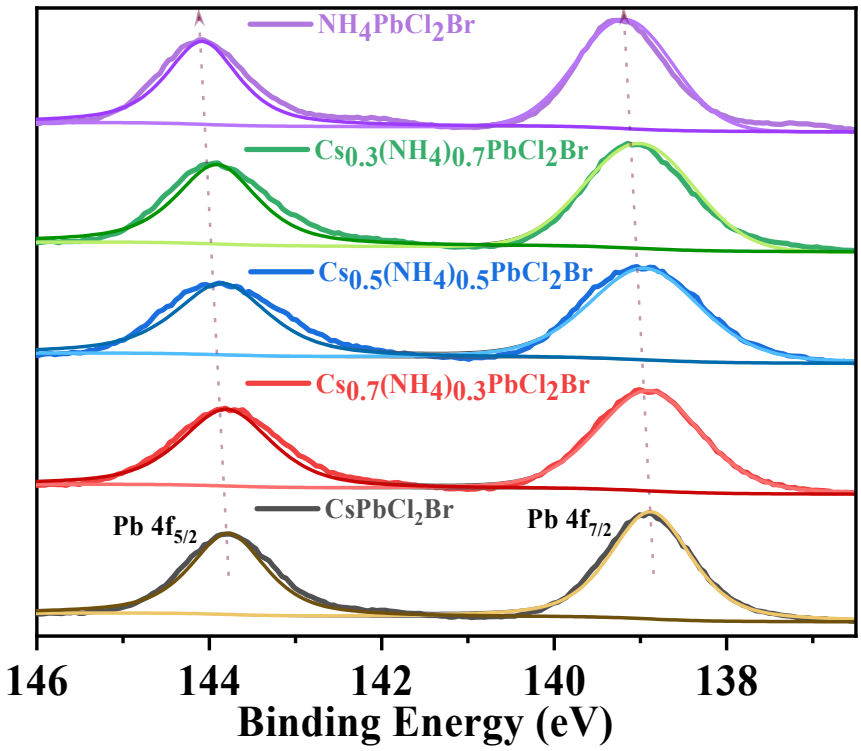

Figure S9. High-resolution Pb 4f XPS spectra of $Cs_x(NH_4)_{1-x}PbCl_2Br$ (x = 1, 0.7, 0.5, 0.3, 0) powders.

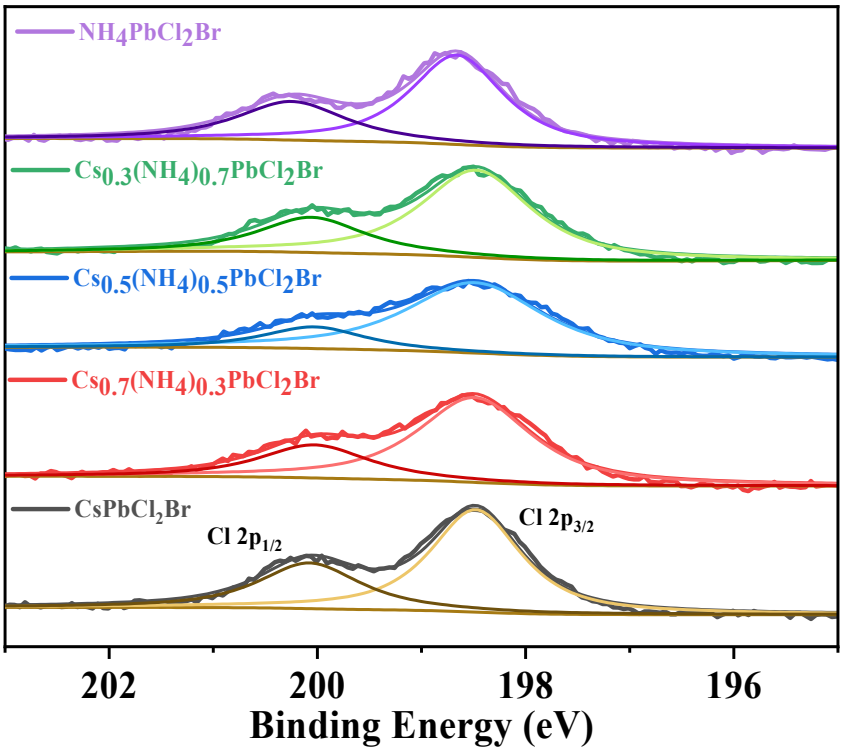

Figure S10. High-resolution Cl 2p XPS spectra of $Cs_x(NH_4)_{1-x}PbCl_2Br$ (x = 1, 0.7, 0.5, 0.3, 0) powders.

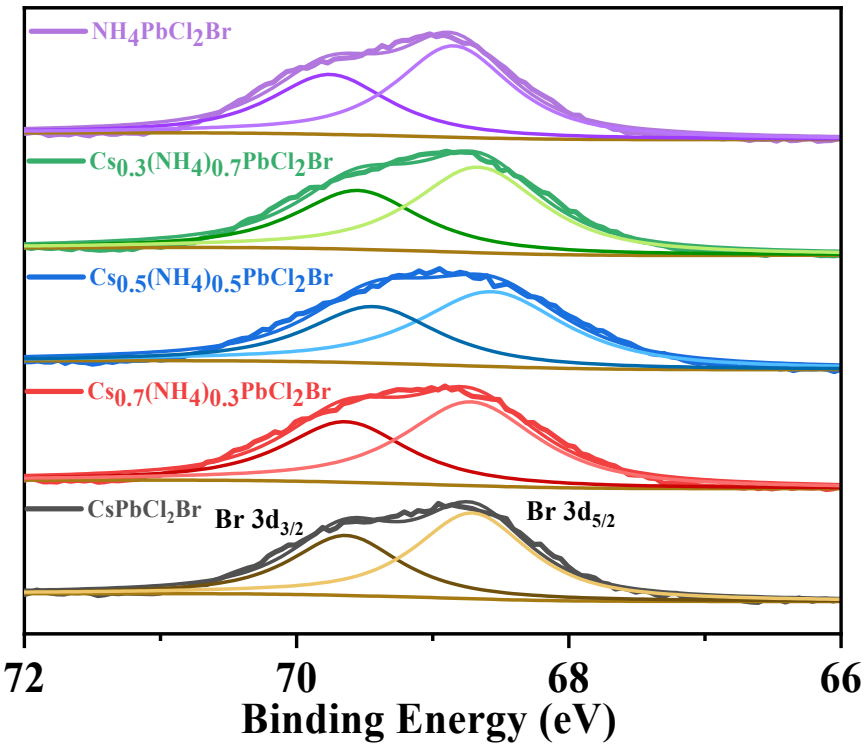

Figure S11. High-resolution Br 3d XPS spectra of $Cs_x(NH_4)_{1-x}PbCl_2Br$ (x = 1, 0.7, 0.5, 0.3, 0) powders.

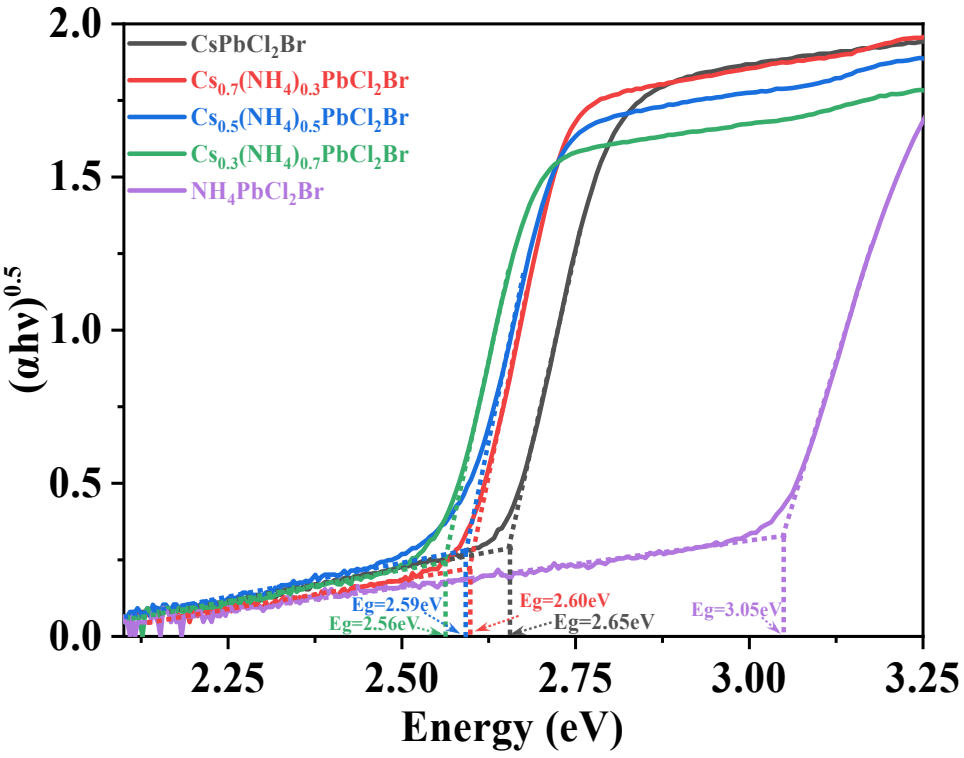

Figure S12. Tauc plots of as-milled $Cs_x(NH_4)_{1-x}PbCl_2Br$ (x = 1, 0.7, 0.5, 0.3, 0) powders.

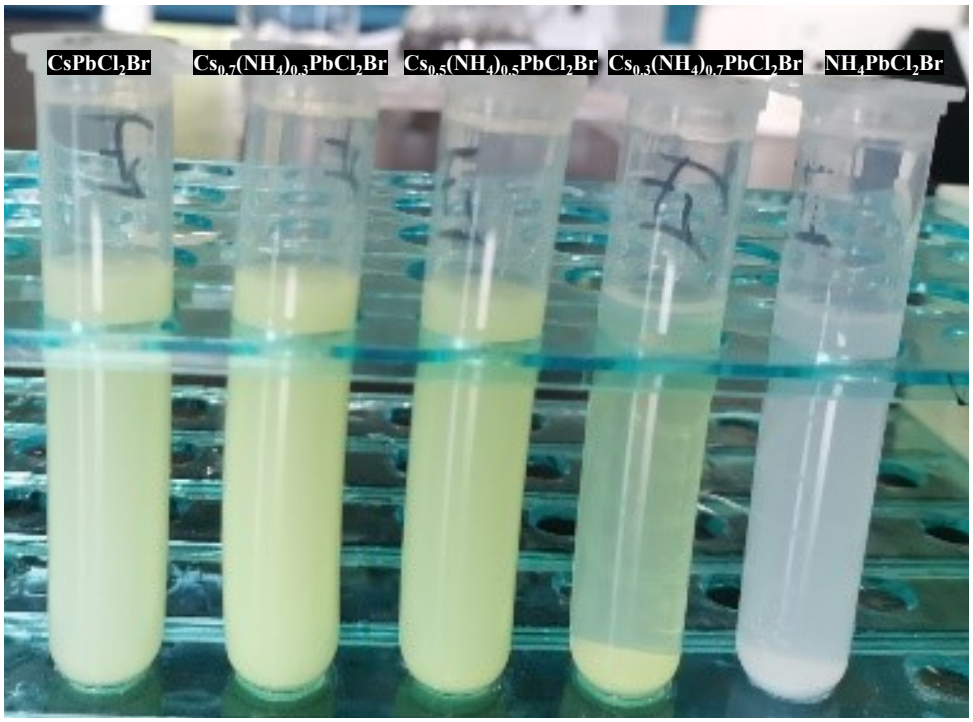

Figure S13. The optical photograph of $Cs_x(NH_4)_{1-x}PbCl_2Br$ (x = 1, 0.7, 0.5, 0.3, 0) powders dispersed in n-hexane solvent before centrifugation.

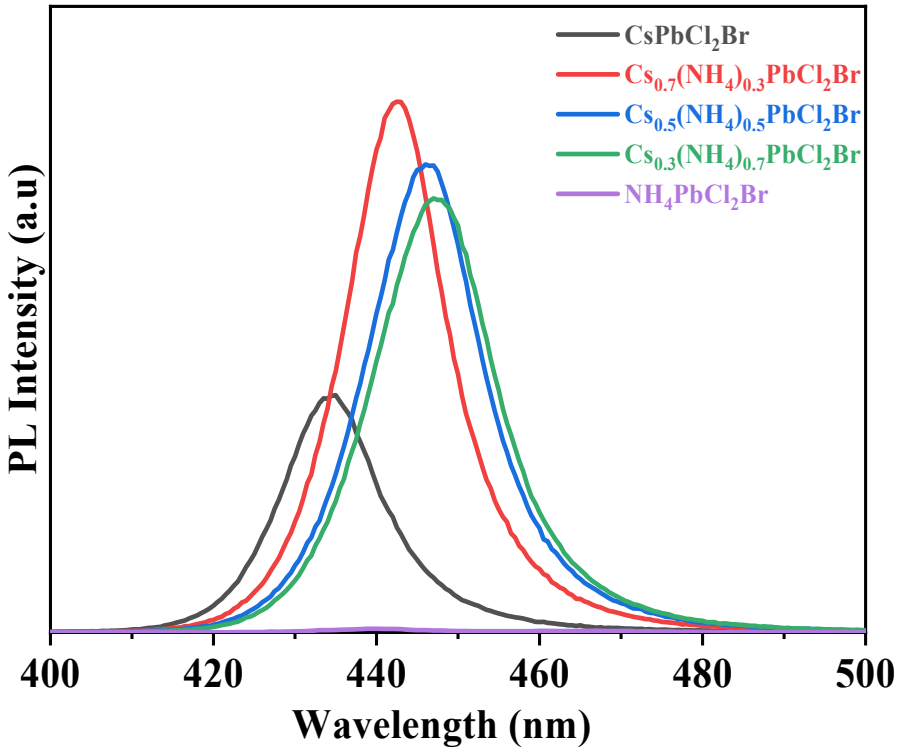

Figure S14. The PL spectra of $Cs_x(NH_4)_{1-x}PbCl_2Br$ (x = 1, 0.7, 0.5, 0.3, 0) NC solutions obtained after centrifugation under UV irradiation (λ_{ex} = 365 nm).

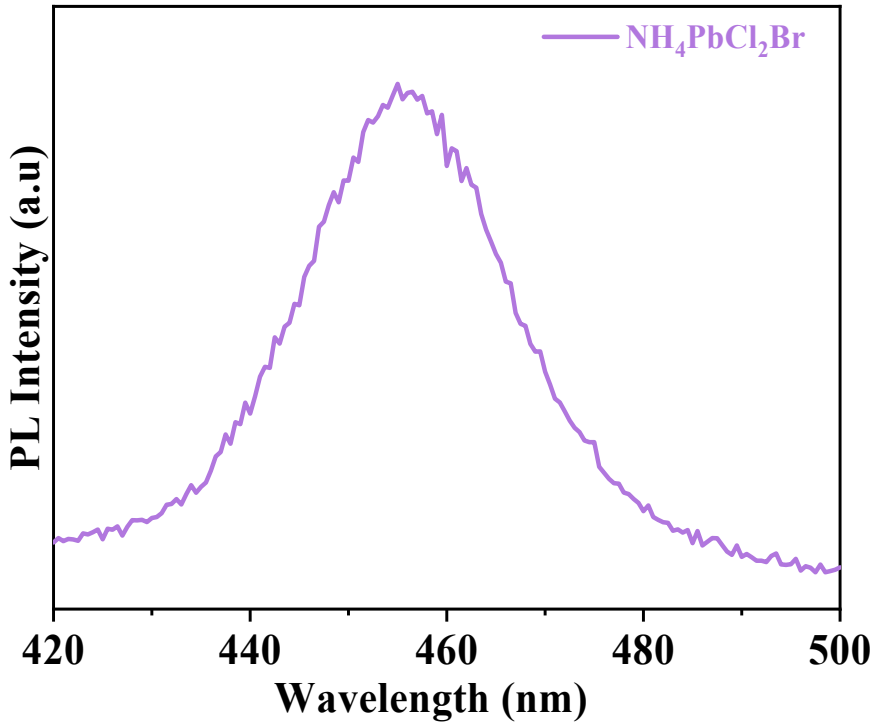

Figure S15. The PL spectra of NH_4PbCl_2Br NC solution measured with the doubled slit width for both excitation and emission (λ_{ex} = 365 nm).

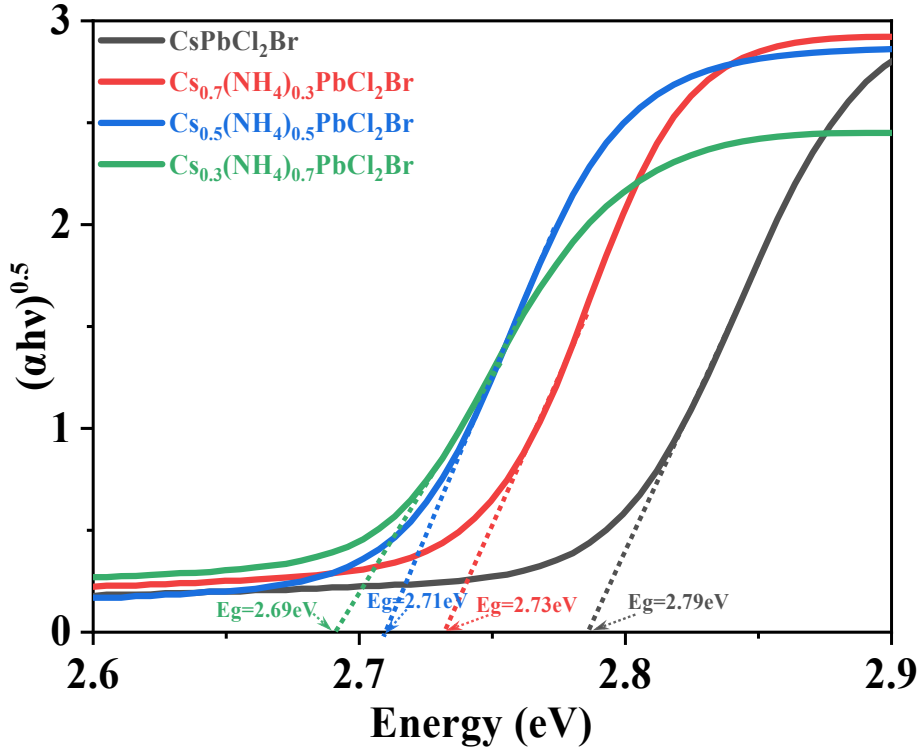

Figure S16. Tauc plots of $Cs_x(NH_4)_{1-x}PbCl_2Br$ (x = 1, 0.7, 0.5, 0.3, 0) NCs.

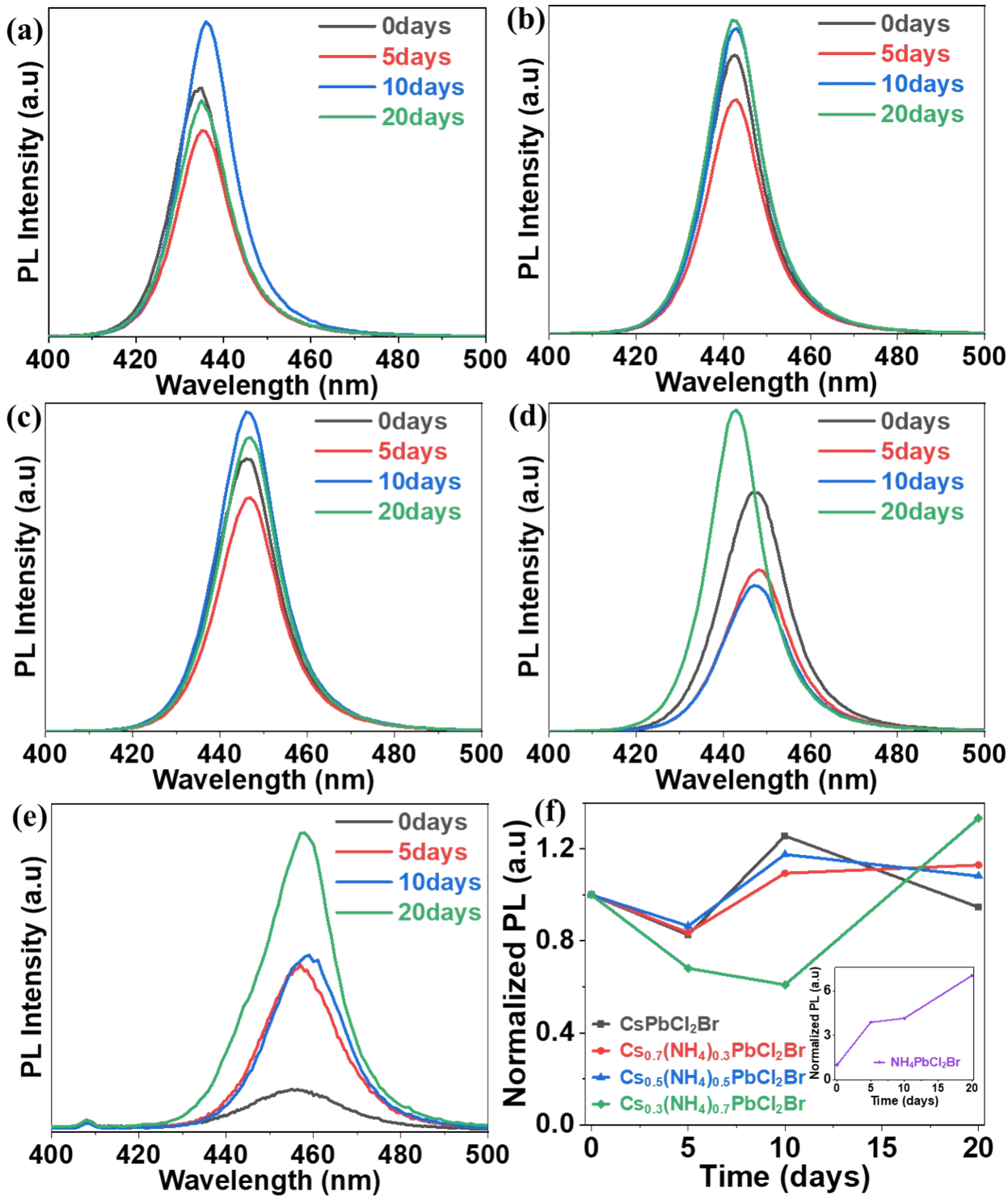

Figure S17. PL spectra of (a) $CsPbCl_2Br$, (b) $Cs_{0.7}(NH_4)_{0.3}PbCl_2Br$, (c) $Cs_{0.5}(NH_4)_{0.5}PbCl_2Br$, (d) $Cs_{0.3}(NH_4)_{0.7}PbCl_2Br$ and (e) NH_4PbCl_2Br NC solutions after stored under ambient conditions for 0-20 days. (f) is the corresponding normalized PL intensity as a function of storing time.

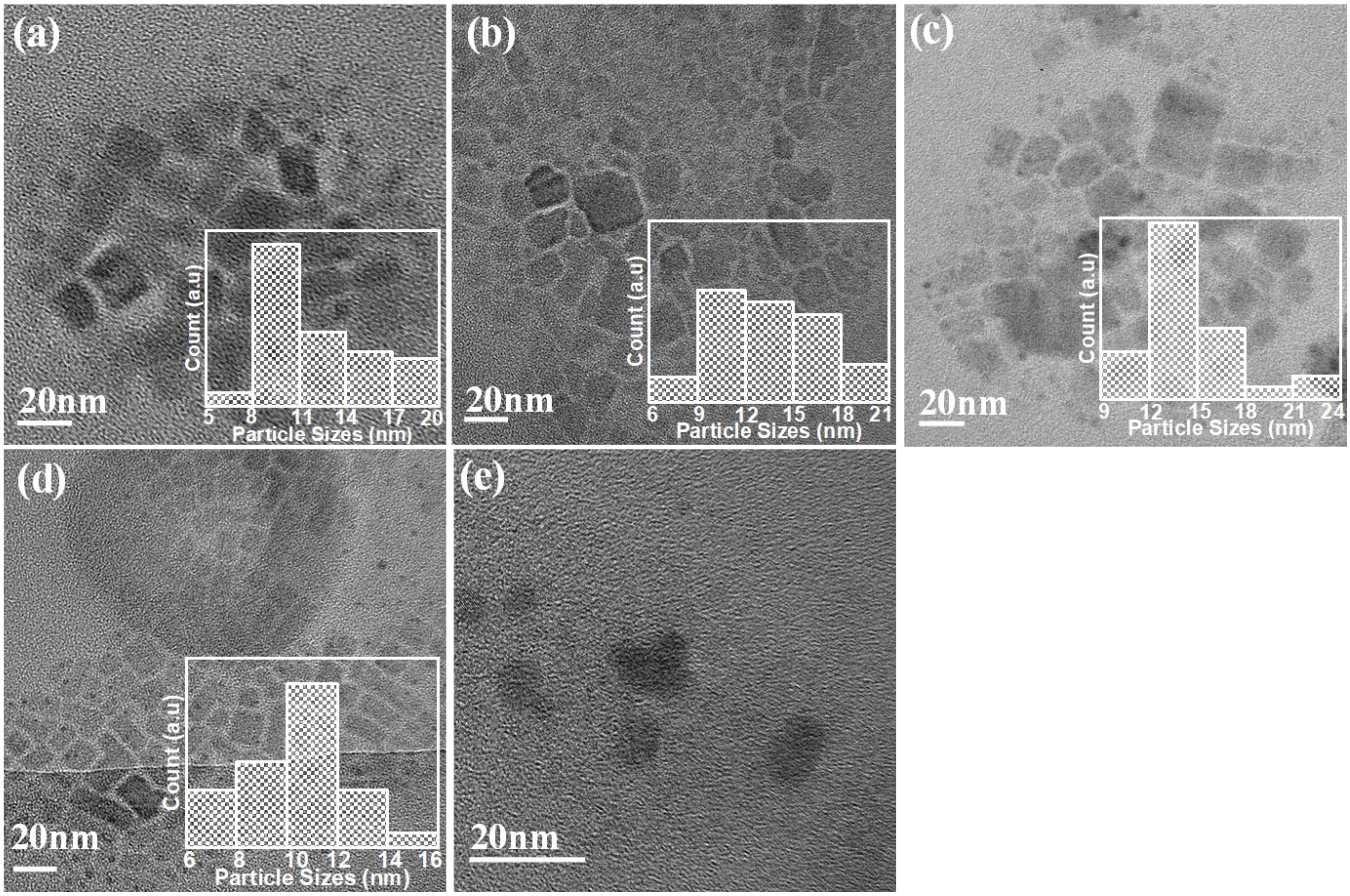

Figure S18. TEM images and the corresponding particles size statistics of (a) $CsPbCl_2Br$, (b) $Cs_{0.7}(NH_4)_{0.3}PbCl_2Br$, (c) $Cs_{0.5}(NH_4)_{0.5}PbCl_2Br$, (d) $Cs_{0.3}(NH_4)_{0.7}PbCl_2Br$ and (e) NH_4PbCl_2Br NCs after being stored under ambient conditions for 29 days. The average sizes are 12.02, 13.19, 15.40 and 10.64 nm for $CsPbCl_2Br$, $Cs_{0.7}(NH_4)_{0.3}PbCl_2Br$, $Cs_{0.5}(NH_4)_{0.5}PbCl_2Br$ and $Cs_{0.3}(NH_4)_{0.7}PbCl_2Br$ NCs, respectively.

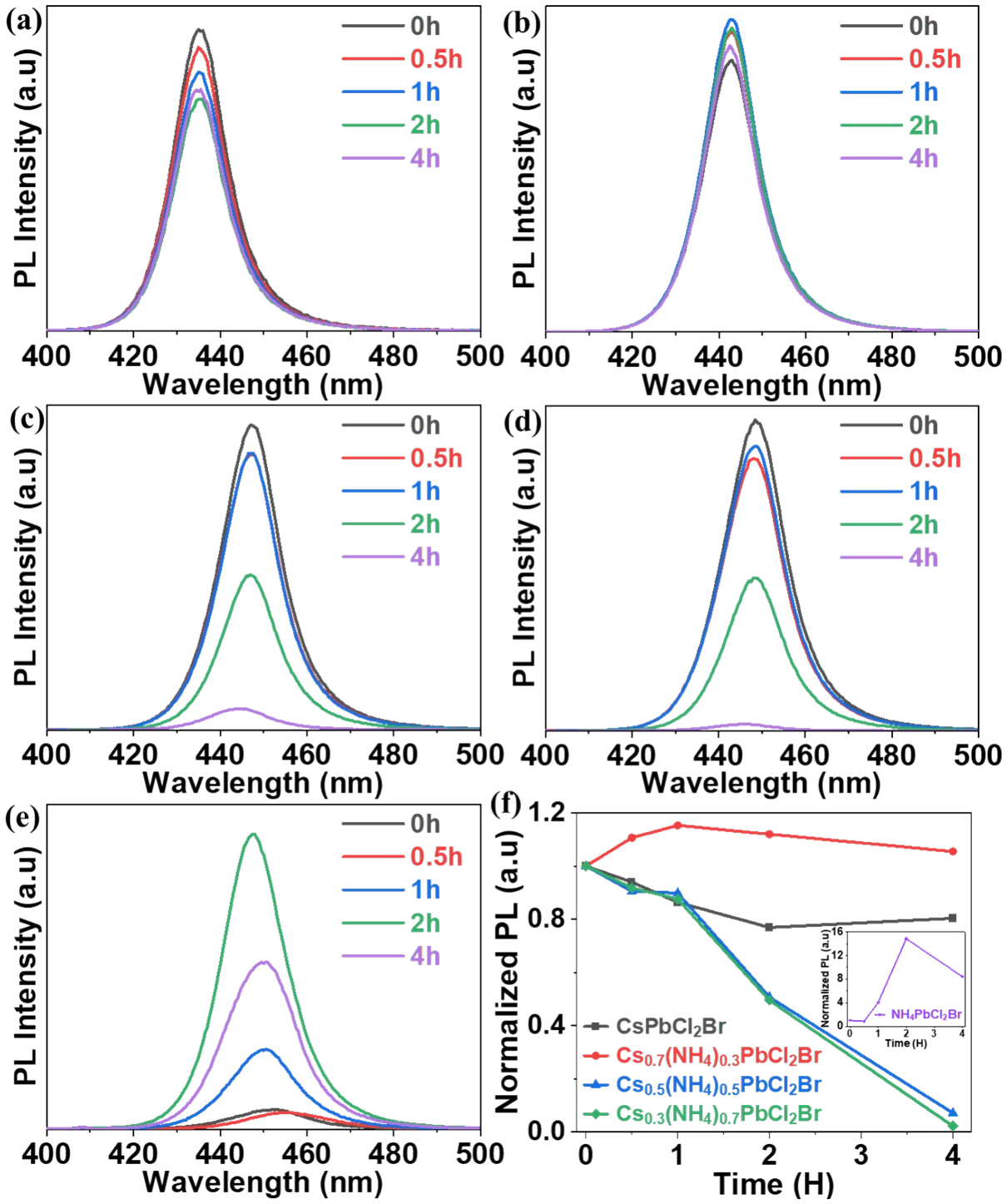

Figure S19. PL spectra of (a) $CsPbCl_2Br$, (b) $Cs_{0.7}(NH_4)_{0.3}PbCl_2Br$, (c) $Cs_{0.5}(NH_4)_{0.5}PbCl_2Br$, (d) $Cs_{0.3}(NH_4)_{0.7}PbCl_2Br$ and (e) NH_4PbCl_2Br NC solutions under continuous 365 nm UV irradiation. (f) is the corresponding normalized PL intensity as a function of UV irradiation time.

Table S1. Detailed PL information of $Cs_x(NH_4)_{1-x}PbCl_2Br$ (x = 1, 0.7, 0.5, 0.3, 0) NCs.

	PL peak (nm)	FWHM (nm)	CIE	Hue
$CsPbCl_2Br$	434	14.45	(0.164, 0.011)	263°
$Cs_{0.7}(NH_4)_{0.3}PbCl_2Br$	443	14.68	(0.160, 0.015)	260°
$Cs_{0.5}(NH_4)_{0.5}PbCl_2Br$	446	16.62	(0.157, 0.018)	259°
$Cs_{0.3}(NH_4)_{0.7}PbCl_2Br$	447	17.44	(0.156, 0.019)	258°
NH_4PbCl_2Br	455	26.31	(0.146, 0.034)	248°

Table S2. Tabulated fitted lifetime components of $Cs_x(NH_4)_{1-x}PbCl_2Br$ (x = 1, 0.7, 0.5, 0.3, 0) NCs.

	τ_3 (ns)	α_3 (%)	τ_2 (ns)	α_2 (%)	τ_1 (ns)	α_1 (%)	τ_{ave} (ns)
$CsPbCl_2Br$	23.10	43.38	4.76	43.57	0.77	13.05	12.20
$Cs_{0.7}(NH_4)_{0.3}PbCl_2Br$	22.89	56.41	5.54	37.71	0.98	5.88	15.06
$Cs_{0.5}(NH_4)_{0.5}PbCl_2Br$	20.97	45.47	5.95	46.42	1.14	8.11	12.39
$Cs_{0.3}(NH_4)_{0.7}PbCl_2Br$	18.15	47.27	4.92	45.03	0.92	7.70	10.87
NH_4PbCl_2Br	19.71	37.95	0.70	20.82	3.54	41.23	9.09